Propeller noise propagation in the sea environment including hull scattering, free surface and seabed effects

Kostas Belibassakis[a], John Prospathopoulos[b]

[a] School of Naval Architecture & Marine Engineering, National Technical University of Athens (NTUA), Heroon Polytechniou 9, 15780 Athens, Greece
[b] School of Mechanical Engineering, National Technical University of Athens (NTUA), Heroon Polytechniou 9, 15780 Athens, Greece

Contact author: Kostas Belibassakis, Fax number: (+30)2107721397,
e-mail: kbel@fluid.mech.ntua.gr

Abstract: *Commercial ships and marine vehicles could contribute significantly to noise in the sea environment, and propeller is considered a main source concerning shipping noise. International Organisations have issued guidelines for the reduction of underwater noise from commercial shipping in order to address adverse impacts on marine life, which has also been identified as an important pollutant and examined under the Marine Strategy Framework (descriptor 11). In this work, we consider the propagation of noise generated by cavitating propellers arranged at the stern of ship/underwater vehicle including the scattering effects by the hull. A Boundary Element Method (BEM) is developed to treat the 3D scattering problem in the frequency domain forced by monopole and dipole source terms associated with the Ffowcs Williams and Hawkings (FW-H) equation, taking into account the free-surface and seabed effects. Numerical results are presented for selected cases illustrating that the hull geometry and acoustic properties, as well as the sea surface and seabed effects are important for the noise level from the above sources in the ocean environment self-contained.*

Keywords: *marine propellers; noise generation and propagation; scattering and directionality effects; 3D-BEM*

1. INTRODUCTION

Commercial ships contribute significantly to the background noise in the sea. This is due to the fact that the number, size and speed of ships continuously increase leading to increasing

noise levels generated from marine propellers, ship machinery, wave breaking, and other sources. It has been demonstrated that ambient noise levels at low frequencies (below 300 Hz) have been increased by 15-20 dB over the last century [1]. On the side of mitigation measures, IMO [2] has issued guidelines aiming at the reduction of underwater noise from commercial shipping to address adverse impacts on marine life.

The propeller noise dominates at high speeds and is considered as the main contributor to commercial shipping noise, especially under cavitating conditions [3]. The numerical prediction of the unsteady performance of marine propellers with and without cavitation provide us with the basic information and data that are subsequently exploited to study noise generation. The acoustic prediction is based on the time-dependent pressure and sheet cavity volume data that are used as input for the Farassat formulation [4] of the FW-H equation [5]. The methods developed for estimating noise generation from non-cavitating and cavitating marine propellers are distinguished into BEM and CFD; see, e.g., [6]. In most cases the effects of the boundaries as the free-surface and seabed, in conjunction with more complicated sources are very important for the generation and long-range propagation of propeller noise; see, e.g., [7]. An additional factor deals with the scattering effects of the hull, which significantly changes the directionality characteristics of the spectrum.

In this work, focusing on the low-frequency band, the underwater noise generated by marine propellers is estimated using an efficient low-cost BEM numerical model. An unsteady propeller hydrodynamics analysis using a Vortex Lattice Method (VLM) provides the data concerning the time history of cavity volume and blade forces, which are introduced as monopole and dipole sources into a simplified noise prediction model. The hydroacoustic problem is formulated and solved in the frequency domain using the Green's function in the sea acoustic waveguide. Reflective and 3D scattering effects of nearby boundaries of free surface and of the ship hull are considered.

2. FORMULATION OF PREDICTION MODELS

2.1 The hydrodynamic model

The propeller blades are considered to be a set of symmetrically arranged thin blades, rotating with a constant angular velocity about a common axis in an unbounded, incompressible fluid. The presence of extraneous boundaries such as the rudder, the hub and the ship hull, are neglected, except that the last is recognized as the body generating the non-uniform flow field (ship's wake). In the present work the propeller hydrodynamic model in inhomogeneous inflow conditions (ship's wake due to hull's boundary layer) is based on VLM [8]. To account for the effects of trailing vorticity, a free vortex sheet downstream of the blades has been incorporated to the model. In the case of wake models the radial distribution of the hydrodynamic pitch angle, is selected to be given by a simplified formula, in terms of the main geometrical and hydrodynamic parameter. At each time step, first the singularity distributions are calculated, then the velocity is computed and finally the pressure is obtained from Bernoulli's equation. The unsteady forces and moments, including thrust, T, and torque, Q, are calculated by pressure integration on propeller blades [8]. As an example of application, a 5-bladed model propeller is considered, with 70deg skew (KP070) for which detailed experimental data are available in [9]. The basic dimensions are: diameter D=0.25m, pitch/diameter ratio P/D=1.2, expanded area ratio 72.5%. The calculated results of the unsteady hydrodynamic analysis for the non-cavitating and cavitating conditions are presented in Fig.1a concerning the circumferential variation of blade thrust coefficient for the key blade ($K_{t,1}$).

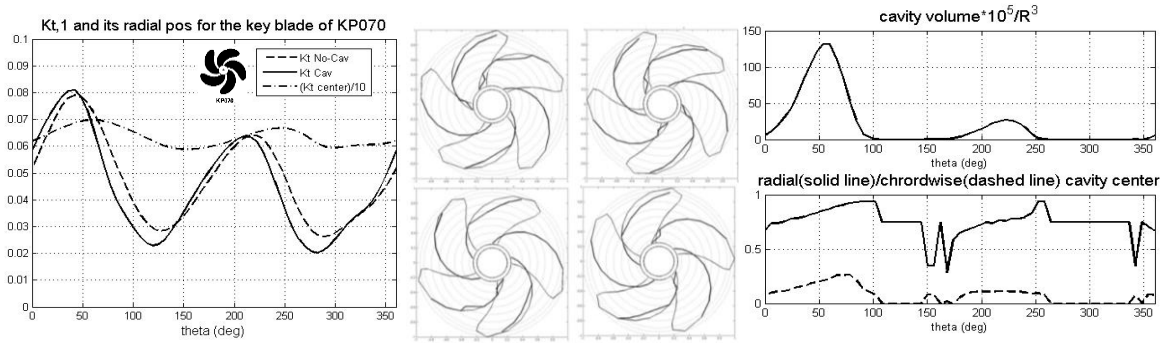

(a) (b) (c)

Fig.1. (a) Circumferential variations of $K_{t,1}$ and radial coordinate of center of blade thrust for the skewed KP070 propeller. (b) Calculated cavitation pattern on the blades. (c) Key blade cavity volume (up) and center of volume (down), as predicted by the present model.

Dashed lines indicate the non-cavitating conditions and solid lines the effect of cavitation. In Fig.1b the calculated cavitation pattern on the blades of the skewed propeller KP070 is presented for various angular positions. Also, the calculated blade cavity volume and the coordinates of its centre are shown in Fig.1c. In general, the present method predictions are found in good agreement with measured data [9].

2.2 The propeller noise prediction model

As propeller rotates in the non-uniform wake, it is subjected to unsteady pressure loads and cavitation which lead to discrete tonal as well as increased broadband noise [6]. Low frequency noise is caused by the fluctuations of blade pressure and variation of unsteady sheet cavitation volume. The former has dipole characteristics and the latter is modelled by a bubble that acts as an acoustic monopole. High-frequency noise is caused by sheet cavity collapse and/or shock wave generation. The acoustic pressure is provided by:

$$\frac{1}{c^2}\frac{\partial^2 p'}{\partial t^2} - \nabla^2 p' = g_m + g_d + g_q\,, \tag{1}$$

where p' denotes the acoustic pressure and c is the speed of sound in the medium (c ranging between 1500m/s and 1550m/s for water); terms in the right-hand side correspond to forcing from the acoustic monopole, dipole and quadrupole source terms respectively. The solution of Eq. (1) is provided by the Farassat formulation. Considering a large distance of the observation point from the propeller and the fact that Mach number is small, the loading and the thickness terms, $p'_L(\mathbf{x},t)$ and $p'_T(\mathbf{x},t)$ respectively, produced by a *Z*-bladed propeller are simplified by

$$p'_L(\mathbf{x},t) \approx -\frac{1}{4\pi c}\sum_{k=1}^{Z}\frac{d\tilde{\mathbf{T}}_{\mathbf{k}}(t_r)}{dt}\frac{\delta\mathbf{x}}{r^2} + \frac{1}{4\pi}\sum_{k=1}^{Z}\tilde{\mathbf{T}}_{\mathbf{k}}(t_r)\frac{\delta\mathbf{x}}{r^3},\ p'_T(\mathbf{x},t) \approx \frac{\rho}{4\pi}\sum_{k=1}^{Z}\frac{d^2V_{c,k}(t_r)}{dt^2}\frac{1}{r}, \tag{2}$$

where $\delta\mathbf{x} = \mathbf{x} - \mathbf{x}_{T,k}(t_r)$, $\mathbf{x}$ is the observation point, $\mathbf{x}_{T,k}(t_r)$ is the thrust centre on the *k*-blade, $r = |\delta\mathbf{x}|$ and $\tilde{\mathbf{T}}_{\mathbf{k}}(t_r)$ is the fluctuating part of the *k*-blade thrust referring to the retarded time $t_r = r/c$. In the $p'_T(\mathbf{x},t)$ formula, $r \approx |\mathbf{x} - \mathbf{x}_{V,k}(t_r)|$ where $\mathbf{x}_{V,k}(t_r)$ is the centre of cavity volume $V_k(t)$ of the *k*-blade. Substitution of the periodic time-series of $\tilde{\mathbf{T}}_{\mathbf{k}}(t_r)$ and $V_k(t)$ by a Fourier series expansion in Eq.(2) leads to the frequency domain form of the FW-H equation:

$$\nabla^2 \tilde{p}(\mathbf{x};\omega_n) + k_n^2 \tilde{p}(\mathbf{x};\omega_n) = V_n\, \delta(\mathbf{x}-\mathbf{x}_0) + X_n\, \frac{\partial}{\partial x}\delta(\mathbf{x}-\mathbf{x}_0)\ , \tag{3}$$

where δ is the Dirac delta function, $\mathbf{x}_0$ stands for the volume and thrust centre, respectively, approximated by the propeller central point. Also, V_n, X_n are the complex monopole and horizontal dipole source intensities, corresponding to the amplitudes of the cavity volume and thrust Fourier expansions, respectively. Using the expression of the Green's function of the Helmholtz equation in free space and its horizontal x-derivative, it is obtained that the acoustic field generated by the above singularities is expressed analytically providing the propeller source incident field $\tilde{p}_i(\mathbf{x},\mathbf{x}_0)$.

2.3 The hydroacoustic model in the frequency domain

Given the intensity of the complex monopole and dipole source terms at the blade frequency and its multiples, as provided by the hydrodynamic propeller responses described above, the scattering problem is considered, excited by any monopole or dipole term in the vicinity of a 3D body representing an AUV or a seagoing vessel, also accounting for the scattering effects of the free-surface and seabed boundary of the ocean acoustic waveguide. The mathematical description of the scattering of time-harmonic waves by an obstacle D leads to a Boundary Value Problem (BVP) for the Helmholtz equation. Considering as an example the boundary of the obstacle ∂D to be acoustically hard, the Neumann boundary condition (BC) is used:

$$\frac{\partial \tilde{p}_S(\mathbf{x})}{\partial n(\mathbf{x})} = -\frac{\partial \tilde{p}_i(\mathbf{x},\mathbf{x}_0)}{\partial n(\mathbf{x})}, \qquad \mathbf{x} \in \partial D\,, \tag{4}$$

where $\mathbf{n}(\mathbf{x})$ is the unit vector normal to ∂D with a direction towards the exterior of D. In the case of the acoustic waveguide, $\tilde{p}_S(\mathbf{x})$ should also satisfy the Dirichlet BC, $\tilde{p}_S = 0$ at the sea surface, $z = 0$, and the Neumann BC, $\partial \tilde{p}_S / \partial n = 0$ at the hard sea bottom, $z = -h$. The solution of the scattering problem is given by the integral

$$\tilde{p}_S(\mathbf{x}) = \int_{\partial D} G(\mathbf{x},\mathbf{y})\,\sigma(\mathbf{y})\,dS(\mathbf{y}), \qquad \mathbf{x} \in R^3 \setminus \partial D\,, \tag{5}$$

where $G(\mathbf{x},\mathbf{y})$ is the Green's function of the Helmholtz equation in the waveguide, given by either by a normal series expansion [10], or by a superposition of fields of monopole sources according to the image theory. The distribution of source intensities on the body surface, $\sigma(\mathbf{y})$, is provided as the solution of the BVP, discretized and solved using a 3D BEM. More details can be found in [11].

3. NUMERICAL RESULTS AND DISCUSSION

The developed BEM is applied to the solution of the scattering problem and the prediction of the acoustic field in the case of noise emission from the propeller of two vessels, a travelling ship and a submerged AUV. In both cases, an isovelocity $c = 1500$ m/s ocean acoustic waveguide of depth $h = 500$ m is considered. Furthermore, the propeller geometry is based on Kp series [9] and the Froude and cavitation numbers are $F_n = 3$ and $\sigma_n = 3.53$ respectively.

3.1 The case of the surface ship

The hull of the ship is modelled using the standard parabolic Wigley hull geometry, where the length and the breadth are chosen as L=130m and B=25m, respectively, and the draft is taken equal to T= 6m. The horizontal distance of the source (modelling the propeller) from the stern is $0.1L$ and the propeller axis submergence depth is 4.5m. The propeller is a 7-times scaled-up version of the 5-bladed model of Fig.1. The selected Froude number corresponds to a rotational frequency $rps = 3.71\text{Hz}$ and a blade frequency $f_0 = 5 \times rps = 18.57\text{Hz}$. A number of $25 \times 10 = 250$ elements are used for the discretization of the hull in BEM, proven to be enough for the numerical convergence of the results. In Fig.2, the contours of the real part of the acoustic field are compared between the semi-infinite medium and the ocean waveguide cases, for the 3rd harmonic. The effect of the seabed on noise directivity is clearly seen in the right plot. The scattering by the hull increases the sound pressure level at the side of the prow.

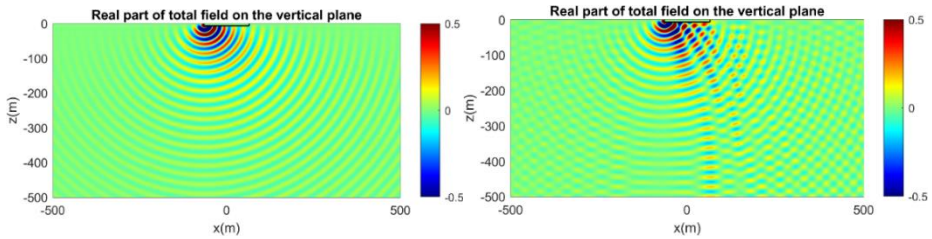

Figure 2: Seabed effect on the acoustic field around the travelling ship for the 3rd harmonic f=55.71Hz. Left column: Semi-infinite medium. Right column: Ocean waveguide.

3.2 The case of the submerged AUV

The hull of the AUV is modelled using the typical Myring geometry, where $L = 7\text{m}$ (and $a = 1.5m$, b =1m, d =0.7m and $n = 3$). The submergence depth is taken as 490m meaning that the AUV is 10m above the seabed. The size of the vessel in this case is significantly smaller (compared to the ship) and its submergence depth is large, therefore focus is made on a smaller region around the AUV hull, close to the seabed. In addition, due to the smaller size of the propeller, the rotational frequency is higher for the same Froude number. As a result, all harmonics are shifted to a higher level. In Fig.3a, the acoustic field around the AUV is shown for the 5th harmonic, with and without (semi-infinite medium) the presence of the seabed. When the effect of the seabed is considered, there is a clear change in the acoustic field around the hull and an increase in the sound pressure level close to the bottom. In comparison to the ship case, the contribution of the dipole term to the total noise level increases. It is seen that, for the fundamental frequency, the contribution of the dipole term is dominant (Fig.3b).

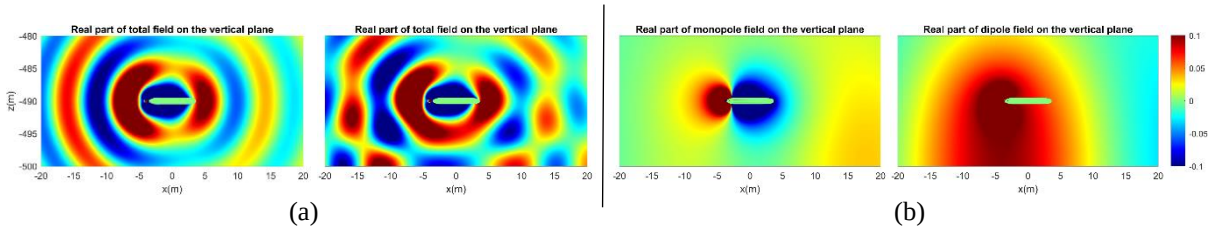

(a) (b)

Figure 3: Real part of acoustic field around the AUV (a)Seabed effect at $f = 5f_0 = 173.71\text{Hz}$ (5th harmonic). Left: Semi-infinite medium. Right: Ocean waveguide. (b)Comparison between monopole (left) and dipole (right) contributions at fundamental frequency $f_0 = 34.74\,\text{Hz}$.

4. CONCLUSIONS

In the present work, the 3D scattering problem in the ocean acoustic waveguide is studied by developing a 3D-BEM model in the frequency domain. Noise is generated by cavitating propellers for a surface ship and a small AUV. The monopole and dipole source terms are derived from the solution of the FW-H equation, which is considered in the frequency domain. The Helmholtz equation takes as input the cavitation and blade loading data and the strength of the acoustic sources is provided by the solution of the hydrodynamic problem in the vicinity of the propeller. The effects of the free surface and the seabed are considered through the corresponding boundary conditions of the 3D scattering problem. In the ship case, results show that the effects of the hull scattering, the seabed and the sea surface are important for the directionality of the generated noise. In the AUV case, due to the larger submergence depth, the effect of the free surface is weak, and the directionality of the propeller noise is mainly affected by the body scattering and the presence of the seabed. This result may be further exploited to investigate long-range propagation of the acoustic spectrum in the ocean waveguide at various azimuthal directions, and support the optimization of software tools for the estimation of the shipping noise footprint over extended geographical areas; see, e.g., [12].

REFERENCES

[1] **McKenna, M., Ross, D., Wiggins, S., Hildebrand**, **J.**. Underwater radiated noise from modern commercial ships, *J Acoust Soc Am.*, 131(1), pp.92-103, 2012.

[2] **IMO**, *Guidelines for the Reduction of Underwater Noise from Commercial Shipping to Address Adverse Impacts on Marine Life* London, 2014.

[3] **Wittekind, D., Schuster, M.**, Propeller cavitation noise and background noise in the sea, *Ocean Engineering* 120, pp.116-121, 2016

[4] **Farassat, F.,**. Acoustic Radiation from Rotating Blades - the Kirchoff method in aeroacoustics, *J.Sound Vib.*, 239, pp.785-800, 2001, doi:10.1006/jsvi.2000.3221

[5] **Ffowcs Williams, J.E., and D.L. Hawkings**, Sound Generated by Turbulence and Surfaces in Arbitrary Motion, *Philos. Trans. R. Soc*. 264, pp.321–342, 1969.

[6] **Seol, H., Suh, J.C., Lee, S.**, Development of hybrid method for the prediction of underwater propeller noise, *Journal of Sound and Vibration*, 288, pp.345–360, 2005.

[7] **Petris, G., Cianferra, M., Armenio, V.,** Marine propeller noise propagation within bounded domains, *Ocean Engineering*, 265, 112618, 2022.

[8] **Belibassakis, K.** Generation and propagation of underwater noise from marine propellers, *Proc Int. Conf Euronoise 2018*, Crete, pp.2825-2834, 2018.

[9] **Kim, K.H., Nguyen, P.N.**, Propeller Cavitation and Cavitation-Induced Pressure Fluctuation: Correlation Between Theory and Experiments, *Proc. SNAME Propellers '88 Symposium*, Virginia Beach, Virginia, USA, 1988, doi: 10.5957/PSS-1988-10.

[10] **Jensen, F.B., Kuperman, W.A., Porter, M.B., Schmidt, H.**, *Computational Ocean Acoustics*, 2nd edition, Springer New York, 2011.

[11] **Belibassakis K, Prospathopoulos J, Malefaki I**, Scattering and Directionality Effects of Noise Generation from Flapping Thrusters Used for Propulsion of Small Ocean Vehicles MDPI *J. Marine Science and Engineering* 10 (8), 1129, 2022

[12] **Athanassoulis, G., Belibassakis, K., Gerostathis T., Prospathopoulos, A.**, A software tool for estimating shipping noise footprint with application to South Adriatic – Ionian Sea. *Proc. Int. Conf. Euronoise 2018,* Crete, pp.2835-2842, 2018.